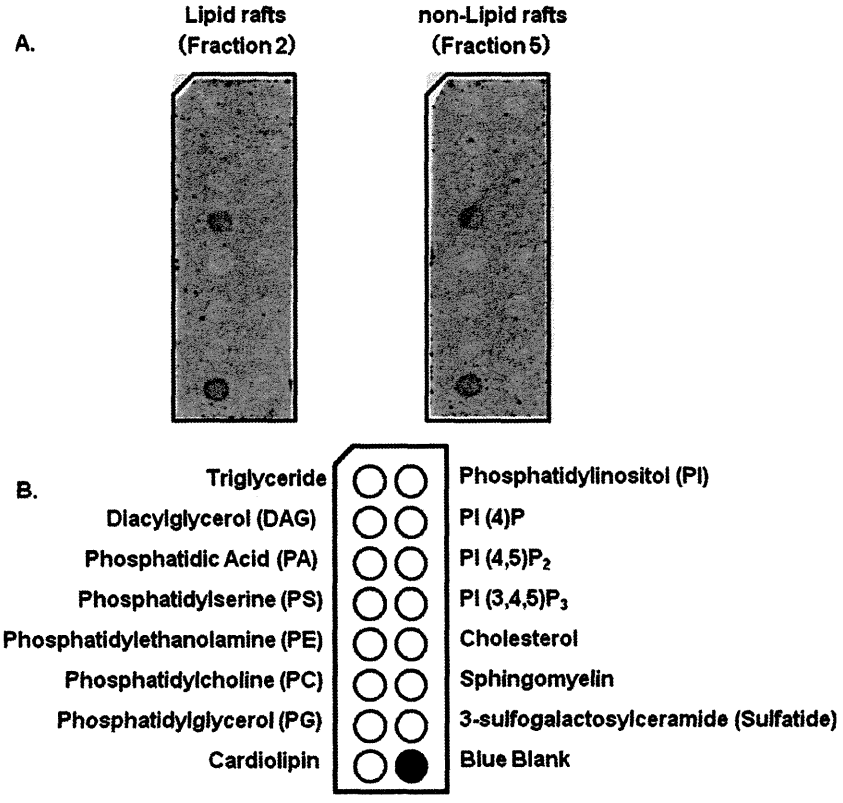

Fig. 5. Interaction of NEP with various lipids. Lipid-attached membrane was treated with sucrose density fractions of SH-SY5Y neuronal cells. After incubation and washing, the membrane was incubated with anti-NEP monoclonal antibody as described in Materials and Methods. The bound NEP was detected by ECL advance. **A:** ECL results. **B:** Lipids attached to the membrane.

Direct Inteaction of NEP With Lipids

The results described above suggest that NEP is localized in lipid rafts, possibly by its direct association with cholesterol. Finally, interaction of NEP with lipids was investigated by using lipid-spotted P-6002 membrane. Fractionated rafts (fraction 2 in Fig. 1A) and nonrafts fractions (fraction 5 in Fig. 1A) were concentrated by ultracentrifugation and incubated with lipids. After washing of the P-6002 membrane, lipid-bound NEP was detected by the specific antibody. Unexpectedly, NEP both in lipid rafts and in nonrafts fractions interacted with phosphatidylserine and cardiolipin but not with cholesterol (Fig. 5).

DISCUSSION

In this study, we found that only the mature form of NEP, glycosylated in the Golgi, and not the immature form, residing in the ER, was localized in lipid rafts (Fig. 1A,B). This indicates that complete glycosylation is required for the association of NEP with lipid rafts. Two possible explanations for this were considered. One is that maturation may be necessary for NEP to bind to a carrier protein such as a glycosylphosphatidylinositol (GPI)-anchored protein. The other is that a small conformational change caused by maturation increases the affinity of NEP for molecules found in lipid rafts, such as sphingolipids and cholesterol. With regard to the former, there have been several reports concerning carrier proteins. One study found that, when the transmembrane and C-terminal domains of BACE1 were replaced with a GPI anchor signal sequence, it was translocated to lipid rafts (Cordy et al., 2003). Another study found that the addition of the N-terminal domain of growth-associated protein 43 (GAP43) to the N-terminus of NEP increased the amount of NEP present in lipid rafts by 1.3-fold (Hama et al., 2004). With regard to the latter possible explanation, we found evidence that the localization of the mature form of NEP in lipid rafts was dependent on the content of cholesterol (Figs. 2, 3). Interestingly, although NEP was completely delocalized by cholesterol depletion, flotillin-1, a lipid raft marker, was not delocalized from lipid rafts by treatment with MβCD (Fig. 2). In this regard, flotillin-1 has been reported to be enriched in detergent-resistant microdomains that are MβCD resistant, although the mechanism

remains to be investigated (Rajendran et al., 2003). Moreover, to examine whether the delocalization of NEP from lipid rafts was caused by its direct association with cholesterol, we extracted lipid raft membranes and treated them with MβCD in vitro (Fig. 3). Consistently with the results presented in Figure 2, NEP was delocalized from lipid rafts membrane by cholesterol depletion, although not completely so (Fig. 3). The difference in the efficiency of NEP delocalization between cell and cell-free systems may be caused by the different conditions used (reaction temperature, membrane state, effects of ultracentrifugation). We conclude that the localization of mature NEP in lipid rafts depends on their cholesterol content.

We investigated the direct association of NEP with pure phospholipids and cholesterol (Fig. 5). Both NEP in rafts and nonrafts directly interacted with phosphatidylserine and cardiolipin. Cardiolipin is a major phospholipid of inner membrane of mammalian mitochondria, so phosphatidylserine might be the major interactor of NEP in lipid rafts. Moreover, immunocytochemical analysis showed that the clustered localization of endogenous NEP in SH-SY5Y cells became dispersed after MβCD treatment (Supp. Info. Fig. 1). Therefore, we conclude that NEP directly associated with phosphatidylserine in cholesterol-rich lipid rafts and MβCD-induced cholesterol depletion triggers the destruction of lipid composition and releases the NEP from rafts. However, the protease activities of mature NEP were unexpectedly comparable in lipid raft and nonlipid raft fractions, as assessed by *p*-NA peptide assay. It is possible that the fractionated lipid rafts did not reflect intracellular conditions (Pike, 2004). However, this result suggests that the association with lipid rafts does not itself modify the protease activity of NEP.

Considering the localization of Aβ in lipid rafts through association with cholesterol (Kakio et al., 2002), we hypothesized that the localization of mature NEP in lipid rafts facilitated its association with Aβ and thereby altered Aβ degradation. Recent studies have shown that lipid raft-dependent endocytosis is the predominant Aβ uptake mechanism (Lai and McLaurin, 2011), that there are correlations between memory deficits and intracellular Aβ levels in several mouse AD models (Billings et al., 2005; Knobloch et al., 2007; Bayer and Wirths, 2008), and that intracellular Aβ level correlates with extracellular amyloid deposition (Yang et al., 2011). Thus, it seems reasonable to conclude that NEP is localized and active in lipid rafts. Indeed, NEP is detected primarily in presynapses and on or around axons in the hippocampal formation (Fukami et al., 2002), and presynaptic NEP efficiently degrades Aβ (Iwata et al., 2004). Considering these findings, together with the fact that the ϵ4 allele of apolipoprotein E (apoE) is a risk factor in nonfamilial AD (Kim et al., 2009), we suggest that cholesterol, overloaded by aging or a high-fat diet, enlarges the area occupied by lipid rafts, thereby decreasing the likelihood of NEP and Aβ coming into contact with each other. As a result, Aβ becomes more abundant, oligomerizes, and causes memory deficits. However, it should be noted that cholesterol itself is a crucial contributor to synaptic structure and function. It has been reported that brain-derived neurotrophic factor (BDNF)-dependent cholesterol biosynthesis plays an important role in synapse development (Suzuki et al., 2007). It would therefore be important to maintain normal cholesterol metabolism during AD therapy.

We further investigated the effects of dimerization on the localization of NEP in lipid rafts. We introduced the E403C mutation into human NEP for the first time. The mutation was originally discovered in rabbit NEP, in which it causes the formation of a covalent homodimer (rabbit NEP normally exists as a monomer). Our results show that human NEP E403C, like rabbit NEP E403C, forms a covalent homodimer. In contrast, human NEP WT, like porcine NEP WT (Kenny et al., 1983), forms a noncovalent homodimer (Fig. 4A,B). Moreover, the noncovalent human NEP WT homodimer, though not resistant to NP-40 or Triton X-100, was resistant to DDM and digitonin. DDM and digitonin dissolve proteins modestly, so the complex remained intact after treatment with these detergents. Interestingly, the localization of mature NEP to lipid rafts was enhanced by its homodimerization (Fig. 4D). With regard to the endopeptidase activity of NEP E403C, Vmax/Km for this mutant was decreased by 50% compared with that for wild-type by using either [D-Ala^2, Leu^5] enkephalin or Suc-Ala-Ala-Leu-NH-Np as a substrate (Hoang et al., 1997). Although the NEP E403C mutant seems to be artificial and to have no physiological significance, these results imply that the protease activity of NEP might be modulated by its dimerization.

In conclusion, we have shown that cholesterol regulates the localization of mature NEP in lipid rafts, where its substrate, Aβ, accumulates. Cholesterol does not, however, modulate the protease activity of NEP.

ACKNOWLEDGMENTS

We thank Dr. Nobuhisa Iwata (Nagasaki University) for providing the protocol for the assay of neprilysin-dependent neutral endopeptidase activity.

REFERENCES

Angelisova P, Drbal K, Horejsi V, Cerny J. 1999. Association of CD10/neutral endopeptidase 24.11 with membrane microdomains rich in glycosylphosphatidylinositol-anchored proteins and Lyn kinase. Blood 93:1437–1439.

Bayer TA, Wirths O. 2008. Review on the APP/PS1KI mouse model: intraneuronal Abeta accumulation triggers axonopathy, neuron loss and working memory impairment. Genes Brain Behav 7(Suppl 1):6–11.

Billings LM, Oddo S, Green KN, McGaugh JL, LaFerla FM. 2005. Intraneuronal Abeta causes the onset of early Alzheimer's disease-related cognitive deficits in transgenic mice. Neuron 45:675–688.

Cordy JM, Hussain I, Dingwall C, Hooper NM, Turner AJ. 2003. Exclusively targeting beta-secretase to lipid rafts by GPI-anchor addition up-regulates beta-site processing of the amyloid precursor protein. Proc Natl Acad Sci U S A 100:11735–11740.

Fukami S, Watanabe K, Iwata N, Haraoka J, Lu B, Gerard NP, Gerard C, Fraser P, Westaway D, St. George-Hyslop P, Saido TC. 2002.

Abeta-degrading endopeptidase, neprilysin, in mouse brain: synaptic and axonal localization inversely correlating with Abeta pathology. Neuroscience research 43:39–56.

Hama E, Shirotani K, Iwata N, Saido TC. 2004. Effects of neprilysin chimeric proteins targeted to subcellular compartments on amyloid beta peptide clearance in primary neurons. J Biol Chem 279:30259–30264.

Hardy JA, Higgins GA. 1992. Alzheimer's disease: the amyloid cascade hypothesis. Science 256:184–185.

Hellstrom-Lindahl E, Ravid R, Nordberg A. 2008. Age-dependent decline of neprilysin in Alzheimer's disease and normal brain: inverse correlation with A beta levels. Neurobiol Aging 29:210–221.

Hoang MV, Sansom CE, Turner AJ. 1997. Mutagenesis of Glu403 to Cys in rabbit neutral endopeptidase-24.11 (neprilysin) creates a disulphide-linked homodimer: analogy with endothelin-converting enzyme. Biochem J 327:925–929.

Iwata N, Tsubuki S, Takaki Y, Shirotani K, Lu B, Gerard NP, Gerard C, Hama E, Lee HJ, Saido TC. 2001. Metabolic regulation of brain Abeta by neprilysin. Science 292:1550–1552.

Iwata N, Takaki Y, Fukami S, Tsubuki S, Saido TC. 2002. Region-specific reduction of A beta-degrading endopeptidase, neprilysin, in mouse hippocampus upon aging. J Neurosci Res 70:493–500.

Iwata N, Mizukami H, Shirotani K, Takaki Y, Muramatsu S, Lu B, Gerard NP, Gerard C, Ozawa K, Saido TC. 2004. Presynaptic localization of neprilysin contributes to efficient clearance of amyloid-beta peptide in mouse brain. J Neurosci 24:991–998.

Kakio A, Nishimoto S, Yanagisawa K, Kozutsumi Y, Matsuzaki K. 2002. Interactions of amyloid beta-protein with various gangliosides in raft-like membranes: importance of GM1 ganglioside-bound form as an endogenous seed for Alzheimer amyloid. Biochemistry 41:7385–7390.

Kanemitsu H, Tomiyama T, Mori H. 2003. Human neprilysin is capable of degrading amyloid beta peptide not only in the monomeric form but also the pathological oligomeric form. Neurosci Lett 350:113–116.

Kawarabayashi T, Shoji M, Younkin LH, Wen-Lang L, Dickson DW, Murakami T, Matsubara E, Abe K, Ashe KH, Younkin SG. 2004. Dimeric amyloid beta protein rapidly accumulates in lipid rafts followed by apolipoprotein E and phosphorylated tau accumulation in the Tg2576 mouse model of Alzheimer's disease. J Neurosci 24:3801–3809.

Kenny AJ, Fulcher IS, McGill KA, Kershaw D. 1983. Proteins of the kidney microvillar membrane. Reconstitution of endopeptidase in liposomes shows that it is a short-stalked protein. Biochem J 211:755–762.

Kim J, Basak JM, Holtzman DM. 2009. The role of apolipoprotein E in Alzheimer's disease. Neuron 63:287–303.

Knobloch M, Konietzko U, Krebs DC, Nitsch RM. 2007. Intracellular Abeta and cognitive deficits precede beta-amyloid deposition in transgenic arcAbeta mice. Neurobiol Aging 28:1297–1306.

Kojro E, Gimpl G, Lammich S, Marz W, Fahrenholz F. 2001. Low cholesterol stimulates the nonamyloidogenic pathway by its effect on the alpha-secretase ADAM 10. Proc Natl Acad Sci U S A 98:5815–5820.

Lafrance MH, Vezina C, Wang Q, Boileau G, Crine P, Lemay G. 1994. Role of glycosylation in transport and enzymic activity of neutral endopeptidase-24.11. Biochem J 302:451–454.

Lai AY, McLaurin J. 2011. Mechanisms of amyloid-beta peptide uptake by neurons: the role of lipid rafts and lipid raft-associated proteins. Int J Alzheimers Dis 2011:548380.

Matsuzaki K, Noguch T, Wakabayashi M, Ikeda K, Okada T, Ohashi Y, Hoshino M, Naiki H. 2007. Inhibitors of amyloid beta-protein aggregation mediated by GM1-containing raft-like membranes. Biochim Biophys Acta 1768:122–130.

Pike LJ. 2004. Lipid rafts: heterogeneity on the high seas. Biochem J 378:281–292.

Pike LJ. 2006. Rafts defined: a report on the Keystone Symposium on Lipid Rafts and Cell Function. J Lipid Res 47:1597–1598.

Rajendran L, Masilamani M, Solomon S, Tikkanen R, Stuermer CA, Plattner H, Illges H. 2003. Asymmetric localization of flotillins/reggies in preassembled platforms confers inherent polarity to hematopoietic cells. Proc Natl Acad Sci U S A 100:8241–8246.

Riemann D, Hansen GH, Niels-Christiansen L, Thorsen E, Immerdal L, Santos AN, Kehlen A, Langner J, Danielsen EM. 2001. Caveolae/lipid rafts in fibroblast-like synoviocytes: ectopeptidase-rich membrane microdomains. Biochem J 354:47–55.

Selkoe DJ. 2002. Alzheimer's disease is a synaptic failure. Science 298:789–791.

Suzuki S, Kiyosue K, Hazama S, Ogura A, Kashihara M, Hara T, Koshimizu H, Kojima M. 2007. Brain-derived neurotrophic factor regulates cholesterol metabolism for synapse development. J Neurosci 27:6417–6427.

von Tresckow B, Kallen KJ, von Strandmann EP, Borchmann P, Lange H, Engert A, Hansen HP. 2004. Depletion of cellular cholesterol and lipid rafts increases shedding of CD30. J Immunol 172:4324–4331.

Wada S, Morishima-Kawashima M, Qi Y, Misono H, Shimada Y, Ohno-Iwashita Y, Ihara Y. 2003. Gamma-secretase activity is present in rafts but is not cholesterol-dependent. Biochemistry 42:13977–13986.

Yang DS, Stavrides P, Mohan PS, Kaushik S, Kumar A, Ohno M, Schmidt SD, Wesson D, Bandyopadhyay U, Jiang Y, Pawlik M, Peterhoff CM, Yang AJ, Wilson DA, St. George-Hyslop P, Westaway D, Mathews PM, Levy E, Cuervo AM, Nixon RA. 2011. Reversal of autophagy dysfunction in the TgCRND8 mouse model of Alzheimer's disease ameliorates amyloid pathologies and memory deficits. Brain 134:258–277.

Neuroscience Letters 525 (2012) 54–59

Contents lists available at SciVerse ScienceDirect

Neuroscience Letters

journal homepage: www.elsevier.com/locate/neulet

The androgen receptor facilitates inhibition of human *dopamine transporter* (*DAT1*) reporter gene expression by HESR1 and HESR2 via the variable number of tandem repeats

Kouta Kanno[a,b,c,1], Shoichi Ishiura[a,*]

[a] *Department of Life Sciences, Graduate School of Arts and Sciences, The University of Tokyo, Japan*
[b] *Department of Biological Sciences, Graduate School of Science, The University of Tokyo, Japan*
[c] *Japan Society for the Promotion of Science, Japan*

HIGHLIGHTS

- Deletion of the VNTR in the DAT reporter gene increase its expression.
- HESR1 and HESR2 inhibit the reporter gene expression via the VNTR.
- The androgen receptor facilitates the inhibition of the DAT reporter by HESRs.

ARTICLE INFO

Article history:
Received 11 May 2012
Received in revised form 10 July 2012
Accepted 11 July 2012

Keywords:
Genetic polymorphism
Dopamine
Transcription factors
Androgen

ABSTRACT

A functional genetic polymorphism in the 3′-untranslated region (UTR) within exon 15 of the human *DAT* gene (*DAT1*) has been described. This 3′-UTR contains a variable number of tandem repeats (VNTR) 40 bp in length; many association studies of psychiatric or developmental disorders with this VNTR have been conducted. We previously demonstrated that HESR1 (the Hairy/enhancer of split related transcriptional factor 1 with YRPW motif) and HESR2 reduced *DAT* reporter gene expression via this 3′-UTR. VNTR allele-dependent altered reporter gene expression was also observed. In the present study, we wanted to clarify the molecular characterization of HESR1 and HESR2, focusing on its *cis*-element and co-factor. Deletion of the VNTR domain increased reporter gene expression both with and without transfection of HESRs, suggesting that the VNTR inhibits *DAT* expression, and is responsive to HESRs. In the presence of transfected androgen receptor (AR), activity of the luciferase reporter with the nine-repeat allele (9r) decreased, while that with the ten-repeat allele (10r), the most frequent in the population, increased significantly. Furthermore, co-expression of HESR1 or HESR2 with AR increased the inhibitory effect of the HESRs. Our data indicate that a functional modification occurs when the HESRs are coupled with AR. This HESR–AR interaction could be the molecular basis of sexual dimorphisms in DAT expression, or other dopamine-related behavioral traits.

1. Introduction

A functional genetic polymorphism in the 3′-untranslated region (UTR) within exon 15 of the human *dopamine transporter* gene (*DAT1*) has been described [19]. This 3′-UTR contains a variable number of tandem repeats (VNTR) domain, which is 40 bp in length (Fig. 1) [19,29]. Polymorphism within this region is associated with neuropsychiatric disorders, including attention deficit hyperactivity disorder (ADHD), Parkinson's disease (PD), alcoholism, and drug abuse [3,5,27,28,30], as well as genotype-dependent alteration of gene expression, both in vivo [5,13,15,20] and in mammalian cell lines [5,8–10,14,21,22,31].

We previously identified and characterized the Hairy/enhancer of split related transcriptional factor 1 with the YRPW motif (HESR1, HEY1) as a *trans*-acting repressor of gene expression that acts through the 3′-UTR of *DAT1* [7,8]. In addition, we showed that another HESR family member, HESR2, inhibited *DAT1* reporter gene expression [16].

Recently, HESR family members have been reported to interact with co-factors [6]. The candidate co-factor we want to focus on is androgen receptor (AR). In a prostate cancer study, HESR1

* Corresponding author at: Department of Life Sciences, Graduate School of Arts and Sciences, The University of Tokyo, 3-8-1, Komaba, Meguro-ku, Tokyo 153-8902, Japan. Tel.: +81 3 5454 6739; fax: +81 3 5454 6739.
E-mail addresses: canno@carazabu.com (K. Kanno), cishiura@mail.ecc.u-tokyo.ac.jp (S. Ishiura).
[1] Present address: Companion Animal Research, School of Veterinary Medicine, Azabu University, Room 303, Bldg 7, 1-17-71 Fuchinobe, Sagamihara, Kanagawa 229-8501, Japan. Tel: +81 42 769 1853; fax: +81 42 850 251.

0304-3940/$ – see front matter © 2012 Elsevier Ireland Ltd. All rights reserved.
http://dx.doi.org/10.1016/j.neulet.2012.07.021

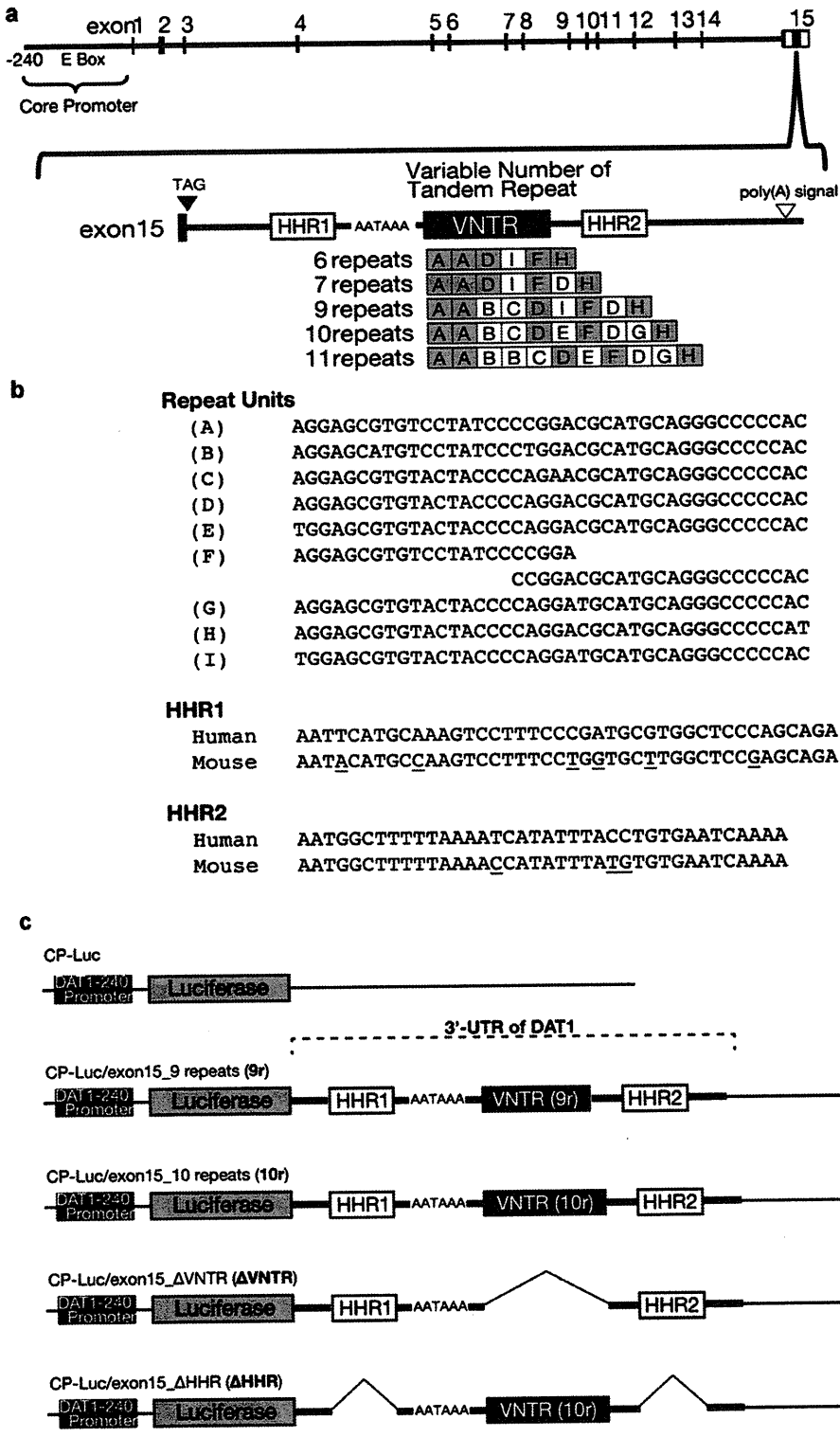

Fig. 1. Structure of the 3′-UTR in *DAT1* and its reporters. (a) The genomic structure of the human *dopamine transporter* (*DAT1*) gene. The coding region (closed box), non-coding region (open box), VNTR domain, and constant parts of the repeat units (gray box) are shown. Exon 15 of *DAT1* contains a stop codon (arrowhead) and polyadenylation signal (open arrowhead). Upstream of the VNTR domain are six nucleotides (AATAAA) that resemble a polyadenylation signal. The allelic variants of the VNTR indicate the repeat unit type (A–I) for each allele. High homology regions (HHR1 and HHR2) between human and mouse are also illustrated. (b) Nucleotide sequence of each unit of the VNTR polymorphism and HHRs in the 3′-UTR of *DAT1*. Bases that differ between human and mouse are underlined. (c) Schematic diagrams of the luciferase reporter vectors used in this study, CP-Luc and four types of CP-Luc/exon15. CP-Luc contains only the *DAT1* core promoter, while each CP-Luc/exon15 contains both the core promoter and 3′-UTR of *DAT1*. CP-Luc/exon15_ΔVNTR and CP-Luc/exon15_ΔHHR are deletion constructs made from CP-Luc/exon15_10 repeats by PCR. VNTR, variable number of tandem repeats and HHR, high homology region between human and mouse 3′-UTR in the DAT gene.

was shown to act as a co-repressor of AR [2]. AR and dopamine are associated with sexual motivation [25]. A sex difference in the disease rate was reported in Parkinson's disease, of which one of the main pathological features is the apoptosis of DA neurons [12]. In addition, DAT expression is lower in males than in females, that is believed to be one reason for the sex difference in the incidence of this disease [23]. Thus, taken together, AR appears to be involved in the dopaminergic system or function of DAT; however, the direct molecular pathway remains unknown. Therefore, the direct pathway of androgen signaling in dopaminergic neurons may be revealed if HESRs are capable of interacting with AR.

While elucidating the HERSs–AR interaction, we wanted to obtain further information regarding the *cis*-element in the 3′-UTR of DAT. There are predicted binding sequences in the 3′-UTR of DAT. Two areas of high homology between humans and mice are located in the non-coding regions. Here, we designate the regions upstream and downstream of the VNTR high homology region 1 (HHR1) and high homology region 2 (HHR2), respectively (Fig. 1). The VNTR domain does not exist in mice, but in our previous study, down-regulation of DAT was observed in Hesr1 knockout (KO) mice at postnatal day zero [7]. Therefore, the elements that the HESRs interact within the 3′-UTR of DAT may or may not be different. To identify these elements, we conducted a reporter assay and observed the effects of HESRs and AR using several DAT luciferase reporter genes.

2. Materials and methods

2.1. Constructs

Four luciferase reporter vectors were prepared (Fig. 1c): CP-Luc/exon15 contained the human *DAT* core promoter and 3′-UTR. CP-Luc, CP-Luc/exon15_10repeats (10r), and CP-Luc/exon15_9repeats (9r) reporter vectors were the same constructs used in our previous studies [8,16].

In the present study, several deletion mutants were prepared. New luciferase reporter gene constructs CP-Luc/exon15_ΔVNTR (ΔVNTR) and CP-Luc/exon15_ΔHHR (ΔHHR) were generated by inverse PCR from the 10r luciferase reporter using primers flanking the deleted regions (Fig. 1c).

The HESR vectors and myc-tagged vector (also used for the empty vector control, VEC) were used in our previous report [19]. The AR expression vector was a gift from Dr. G. Sobue (Nagoya University). Information on the AR vector is included in his work [33].

2.2. Immunocytochemistry

Human neuroblastoma SH-SY5Y cells were plated on collagen-coated cover glasses in 12-well plates, and were transfected with HESR1 or HESR2 and AR ($n=3$). Cells were fixed with 4% paraformaldehyde in PBS for 15 min and washed three times 24 h after transfection.

Cells were then stained with antibodies by standard immunocytochemical process. Images were captured with an All-in-one fluorescence microscope BZ-9000 (Keyence, Osaka, Japan).

2.3. Luciferase reporter assay

Methods used for luciferase activity measurements followed the standard methods of the Dual-Luciferase Reporter Assay System (Promega). The SH-SY5Y cells were transfected with the luciferase reporter gene and each HESR and/or AR or empty vector. Plasmid pRL (Promega) containing the sea pansy (renilla) luciferase gene was co-transfected as a control to normalize for transfection efficiency in all experiments. In the present study, luciferase activities (relative light unit = [values of firefly luc]/[values of renilla]) were standardized to the average of the 10r reporter with VEC group.

2.4. Statistics

All values are reported as the means ± SEM. Student's *t*-test or Tukey–Kramer's honestly significant difference (HSD) test were used as a *post hoc* test after two-way analysis of variance (ANOVA). Differences were considered significant at values of $P<0.05$.

Further information is described in online supplementary information.

3. Results

3.1. Localization of HESR1, HESR2 and AR in SH-SY5Y cells

As shown in Fig. 2, immunoreactivity was observed mainly in the nucleus of cells transfected with HESR1 and HESR2. AR immunoreactivity was also observed in the nucleus.

3.2. Luciferase reporter assay

3.2.1. Effects of putative elements in the 3′-UTR of DAT1

A reporter assay was conducted to identify the effects of each sequence on gene expression with or without transiently expressed HESRs in cultured SH-SY5Y cells using the luciferase reporters illustrated in Fig. 1c.

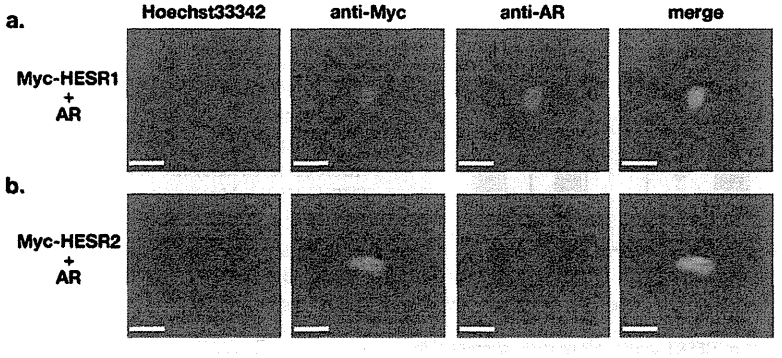

Fig. 2. Cellular localization of transfected HESRs and AR in SH-SY5Y cells. (a) Blue, nucleus; green, Myc-tagged HESR1; and red, androgen receptor (AR). (b) Blue, nucleus; green, Myc-tagged HESR2; and red, AR. Scale bar, 20 μm. (For interpretation of the references to color in this figure legend, the reader is referred to the web version of the article.)

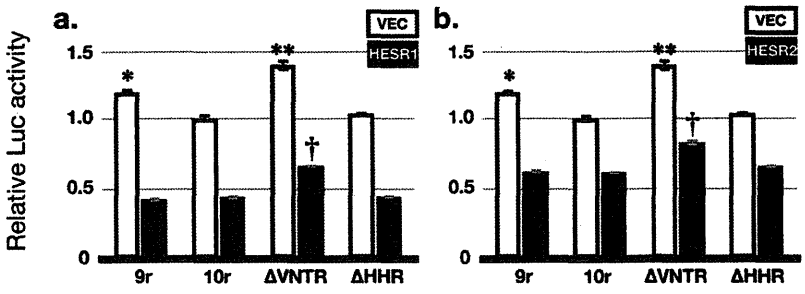

Fig. 3. Regional effects of the *DAT1* 3′-UTR on luciferase reporter activity. Relative luciferase activity of the reporter genes expressed with the empty control vector (a and b), HESR1 (a) or HESR2 (b) in the SH-SY5Y cells are shown. CP-Luc/exon15_9 repeats (9r), CP-Luc/exon15_10 repeats (10r), CP-Luc/exon15_ΔVNTR (ΔVNTR) and CP-Luc/exon15_ΔHHR (ΔHHR) were used. Values represent the means ± SEM. All values were standardized to the 10r with empty vector (VEC) group. *$P<0.05$ vs. the other values of VEC group; **$P<0.01$ vs. the other values of VEC group; and †$P<0.0001$ vs. the other values of HESR1 (a) or HESR2 (b) groups (Tukey–Kramer's HSD test after two-way ANOVA). Comparing the values of HESR1 or HESR2 groups with that of VEC group under each condition of luciferase reporter (9r, 10r, ΔVNTR and ΔHHR), each value of HESR1 or HESR2 groups was significantly lower than that of VEC (Student's *t*-test).

As shown in Fig. 3a, two-way ANOVA indicated a significant effect of transfected factors (VEC and HESR1; $F_{[1,31]}=1855.0$, $P<0.0001$), reporters (9r, 10r, ΔVNTR and ΔHHR; $F_{[3,31]}=82.5$, $P<0.0001$) and interaction of them ($F_{[3,31]}=10.3$, $P=0.0002$). In Fig. 3b, two-way ANOVA also indicated a significant effect of transfected factors (VEC and HESR2; $F_{[1,31]}=792.0$, $P<0.0001$), reporters ($F_{[3,31]}=62.1$, $P<0.0001$) and interaction of them ($F_{[3,31]}=9.5$, $P=0.0003$).

When VEC was co-expressed, the value of 9r was significantly different from the others ($P<0.05$, Fig. 3a and b). Under all conditions, values of ΔVNTR were significantly higher compared to the others in each group (VEC, $P<0.01$, Fig. 3a and b; HESR1 and HESR2, $P<0.0001$, Fig. 3a and 3b, respectively).

3.2.2. *Effects of HESRs and AR on luciferase activity with 9r or 10r*

The effect of AR both with and without HESRs on luciferase activity was examined with either 9r or 10r (Fig. 4). Values of VEC, HESR1 and HESR2 were the same as those in Fig. 3.

Two-way ANOVA indicated significant effect of transfected factors (VEC, AR, HESR1, HESR1 + AR, HESR2 and HESR2 + AR; $F_{[5,47]}=1098.6$, $P<0.0001$). The effect of reporters (9r and 10r) was not significant. However, two-way ANOVA indicated significant interaction of transfected factors and reporters ($F_{[5,47]}=27.5$, $P<0.0001$).

The value of 9r was significantly higher than that of 10r with transfection of VEC while significantly lower with transfection of AR (Student's *t*-test, $P<0.0001$). There was no other significant difference of 9r vs. 10r.

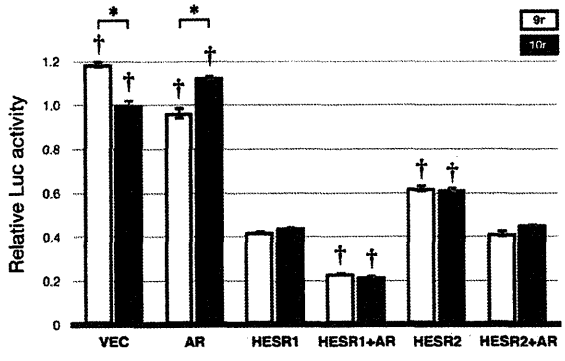

Fig. 4. AR facilitates the inhibitory effect of the HESRs. Relative luciferase activities of the reporter genes were measured when CP-Luc/exon15_9repeats (9r) and CP-Luc/exon15_10repeats (10r) with HESR1 or HESR2, and/or AR were co-expressed in SH-SY5Y cells. Values represent the means ± SEM. *$P<0.0001$, 9r vs. 10r (Student's *t*-test) and †$P<0.0001$ vs. the other values of the same repeats (9r or 10r) group (Tukey–Kramer's HSD test after two-way ANOVA).

Activities of the 9r reporter significantly decreased to 35.5%, 52.3%, and 81.3% upon expression of HESR1, HESR2, or AR, respectively, compared to the empty vector (VEC). Furthermore, luciferase activity with 9r significantly decreased to 19.5% upon co-expression of HESR1 and AR (HESR1 + AR) and to 34.9% with HESR2 + AR. With 10r allele, a similar tendency was observed, but in the presence of AR alone, activity of the 10r reporter significantly increased to 112.6%.

4. Discussion

4.1. *Regional effects of the 3′-UTR in DAT1: an inhibitory role for the VNTR*

It is possible that the 3′-UTR has an inhibitory role in gene expression by comparing the activity of CP-Luc and CP-Luc/exon15, as demonstrated in our previous studies [8,16], but it is unclear whether the VNTR domain itself inhibits DAT expression. To exclude this possibility, we demonstrated that the luciferase activity of ΔVNTR increased compared to that of VNTR-containing reporter genes, suggesting that the VNTR domain itself has a partial inhibitory role and may be a strong candidate *cis*-element for HESRs, even though luciferase activity was reduced in the presence of both HESR1 and HESR2 compared to the VEC control (Fig. 3).

4.2. *Androgen receptor facilitates HESR-mediated inhibition of DAT1 expression*

When designing these experiments, we were inspired by a report on prostate cancer and a VNTR association study. The research of prostate cancer reported that HESR1 is an androgen receptor-interacting factor [2]. It has also been shown that HESR1 is excluded from the nucleus in most human prostate cancers, raising the possibility that abnormal HESR1 subcellular distribution plays a role in the aberrant hormonal responses observed in prostate cancer. However, in the present study, co-localization of HESR1 or HESR2 and AR in the nucleus was observed without any abnormal cellular localization (Fig. 2). Protein expression of HESRs in the nucleus is consistent with data from our previous reports in SH-SY5Y cells and in mouse brain [8,16]. AR expression does not appear to affect HESR localization; however, data of a previous study [2] and ours suggest that HESRs interact with AR in the nucleus via formation of a protein complex, which then down-regulates DAT.

In the present study, we aimed to demonstrate the molecular biological associations among DAT, HESRs and AR. The large decrease in the presence of both HESRs and AR (Fig. 4) appears to be an additive effect, because both HESRs and AR alone exerted an inhibitory effect on the 9r reporter. With 10r

reporter a similar tendency is shown; however, in the presence of AR alone, the activity of the 10r reporter increased to 112.6%. Thus, the coupling of both an inhibitory and facilitative factor resulted in greater inhibition. Therefore, rather than a simple additive effect, a functional modification is believed to occur when the HESRs and AR are coupled, as reported in prostate cancer [2,32].

However, further element analysis of this gene is needed due to the presence of E-box sites in both the mouse and human 3′-UTRs of *DAT*, and because HESR1 and HESR2 may act through the core promoter in the CP-Luc, as shown in our previous report [16]. In any case, since the effect of AR differed depending on the VNTR allele (9r or 10r), the VNTR may be one of the most important elements in this region.

4.3. *A functional consideration: implication for the biological significance of HESRs and AR*

Here, we demonstrated that the interaction between HESRs and AR strongly inhibits the *DAT* reporter gene. Expression of AR in the midbrain dopaminergic regions is detected in the ventral tegmental area (VTA) rather than the substantia nigra (SN) [4]. Additionally, DAT expression is lower in the VTA than in the SN, together with regional differences in electrophysiological properties [18]. The distribution of Hesr1 or Hesr2 did not differ between the regions [16], but Hesrs may contribute to the regional difference in DAT expression by interacting with AR, which localizes specifically in the midbrain. Furthermore, this interaction may be associated with the fact that DAT expression is lower in males than in females [23].

A previous study indicated that the number of sexual partners of the 9r/9r genotype of *DAT1* is fewer than that of 9r/10r or 10r/10r carriers [11]. In Fig. 4, 9r and 10r displayed different responsiveness to AR. This could be the molecular basis for the different number of sexual partners, depending on the VNTR alleles (9r/9r or any 10r) [11] via synaptic tuning of dopamine by DAT, since both dopamine and androgen are strongly involved in sexual motivation [25].

Mutations of the *HESR* genes have not been reported in clinical studies of psychiatric or developmental disorders, but a recent study reported that HESR1 was up-regulated in cell lines derived from patients with an autism spectrum disorder whose disease rate is higher in males [26]. In our study, we demonstrated that the HESRs–AR interaction strongly inhibited *DAT* reporter gene expression. We previously demonstrated that HESR1 having a naturally occurring nonsynonymous SNP at codon 94 (Lue94Met, SNP ID rs11553421) in the HLH domain did not have an ability to repress the DAT reporter gene expression [8]. In addition, this SNP converts HESR1 from an androgen receptor corepressor to co-activator and abolishes HESR1-mediated activation of p53 [32], which has been reported as a schizophrenia susceptibility gene [1]. The VNTR of *DAT1* [3] and DAT expression level [17] are associated to ADHD, of which features are shared with autism spectrum disorder to a certain degree [24]. Taken together, we believe that HESRs together with the VNTR of *DAT1* and AR have important roles in psychiatric disorders, developmental delay and behavioral traits that should be further investigated.

5. Conclusion

We demonstrated that AR facilitates an inhibitory effect of HESR1 and HESR2, which act through the VNTR, on *DAT1* reporter gene expression. Based on these findings, functional analysis of this interaction should be conducted.

Acknowledgements

This work was supported in part by the Human Frontier Science Program and by a Grant-in-Aid from the Ministry of Education, Culture, Sports, Science, and Technology of Japan. K.K. had been supported by a JSPS Research Fellowship for Young Scientists.

We thank Dr. M.J. Bannon (Wayne State University) for kindly providing us with the DAT1-8317 plasmid and Dr. G. Sobue (Department of Neurology, Nagoya University Graduate School of Medicine) for the AR plasmid.

Appendix A. Supplementary data

Supplementary data associated with this article can be found, in the online version, at http://dx.doi.org/10.1016/j.neulet.2012.07.021.

References

[1] N.C. Allen, S. Bagade, M.B. McQueen, J.P. Ioannidis, F.K. Kavvoura, M.J. Khoury, R.E. Tanzi, L. Bertram, Systematic meta-analyses and field synopsis of genetic association studies in schizophrenia: the SzGene database, Nature Genetics 40 (2008) 827–834.
[2] B. Belandia, S.M. Powell, J.M. Garcia-Pedrero, M.M. Walker, C.L. Bevan, M.G. Parker, Hey1, a mediator of notch signaling, is an androgen receptor corepressor, Molecular and Cellular Biology 25 (2005) 1425–1436.
[3] E.H. Cook, M.A. Stein, M.D. Krasowski, N.J. Cox, D.M. Olkon, J.E. Kieffer, B.L. Leventhal, Association of attention-deficit disorder and dopamine transporter gene, American Journal of Human Genetics 56 (1995) 993–998.
[4] L.M. Creutz, M.F. Kritzer, Mesostriatal and mesolimbic projections of midbrain neurons immunoreactive for estrogen receptor beta or androgen receptors in rats, Journal of Comparative Neurology 476 (2004) 348–362.
[5] U.M. D'Souza, I.W. Craig, Functional genetic polymorphisms in serotonin and dopamine gene systems and their significance in behavioural disorders, Progress in Brain Research 172 (2008) 73–98.
[6] A. Fischer, M. Gessler, Delta-Notch-and then? Protein interactions and proposed modes of repression by Hes and Hey bHLH factors, Nucleic Acids Research 35 (2007) 4583–4596.
[7] S. Fuke, N. Minami, H. Kokubo, A. Yoshikawa, H. Yasumatsu, N. Sasagawa, Y. Saga, T. Tsukahara, S. Ishiura, Hesr1 knockout mice exhibit behavioral alterations through the dopaminergic nervous system, Journal of Neuroscience Research 84 (2006) 1555–1563.
[8] S. Fuke, N. Sasagawa, S. Ishiura, Identification and characterization of the Hesr1/Hey1 as a candidate trans-acting factor on gene expression through the 3′ non-coding polymorphic region of the human dopamine transporter (*DAT1*) gene, Journal of Biochemistry 137 (2005) 205–216.
[9] S. Fuke, S. Suo, N. Takahashi, H. Koike, N. Sasagawa, S. Ishiura, The VNTR polymorphism of the human dopamine transporter (*DAT1*) gene affects gene expression, The Pharmacogenomics Journal 1 (2001) 152–156.
[10] T.A. Greenwood, J.R. Kelsoe, Promoter and intronic variants affect the transcriptional regulation of the human dopamine transporter gene, Genomics 82 (2003) 511–520.
[11] G. Guo, Y. Tong, C.W. Xie, L.A. Lange, Dopamine transporter, gender, and number of sexual partners among young adults, European Journal of Human Genetics 15 (2007) 279–287.
[12] C.A. Haaxma, B.R. Bloem, G.F. Borm, W.J. Oyen, K.L. Leenders, S. Eshuis, J. Booij, D.E. Dluzen, M.W. Horstink, Gender differences in Parkinson's disease, Journal of Neurology, Neurosurgery and Psychiatry 78 (2007) 819–824.
[13] A. Heinz, D. Goldman, D.W. Jones, R. Palmour, D. Hommer, J.G. Gorey, K.S. Lee, M. Linnoila, D.R. Winberger, Genotype influences in vivo dopamine transporter availability in human striatum, Neuropsychopharmacology 22 (2000) 133–139.
[14] M. Inoue-Murayama, S. Adachi, N. Mishima, H. Mitani, O. Takenaka, K. Terao, I. Hayasaka, S. Ito, Y. Murayama, Variation of variable number of tandem repeat sequences in the 3′-untranslated region of primate dopamine transporter genes that affects reporter gene expression, Neuroscience Letters 334 (2002) 206–210.
[15] L.K. Jacobsen, J.K. Staley, S. Zoghbi, J.P. Seibyl, T.R. Kosten, R.B. Innis, J. Gelernter, Prediction of dopamine transporter binding availability by genotype: a preliminary report, American Journal of Psychiatry 157 (2000) 1700–1703.
[16] K. Kanno, S. Ishiura, Differential effects of the HESR/HEY transcription factor family on dopamine transporter reporter gene expression via variable number of tandem repeats, Journal of Neuroscience Research 89 (2011) 562–575.
[17] K.H. Krause, S.H. Dresel, J. Krause, C. la Fougere, M. Ackenheil, The dopamine transporter and neuroimaging in attention deficit hyperactivity disorder, Neuroscience and Biobehavioral Reviews 27 (2003) 605–613.
[18] S. Lammel, A. Hetzel, O. Hackel, I. Jones, B. Liss, J. Roeper, Unique properties of mesoprefrontal neurons within a dual mesocorticolimbic dopamine system, Neuron 57 (2008) 760–773.
[19] S.K. Michelhaugh, C. Fiskerstrand, E. Lovejoy, M.J. Bannon, J.P. Quinn, The dopamine transporter gene (SLC6A3) variable number of tandem repeats

domain enhances transcription in dopamine neurons, Journal of Neurochemistry 79 (2001) 1033–1038.
[20] J. Mill, P. Asherson, C. Browes, U. D'Souza, I. Craig, Expression of the dopamine transporter gene is regulated by the 3′-UTR VNTR: evidence from brain and lymphocytes using quantitative RT-PCR, American Journal of Medical Genetics Part B: Neuropsychiatric Genetics 114B (2002) 975–979.
[21] J. Mill, P. Asherson, I. Craig, U.M. D'Souza, Transient expression analysis of allelic variants of a VNTR in the dopamine transporter gene (*DAT1*), BMC Genetics 6 (2005).
[22] G.M. Miller, B.K. Madras, Polymorphisms in the 3′-untranslated region of human and monkey dopamine transporter genes affect reporter gene expression, Molecular Psychiatry 7 (2002) 44–55.
[23] M. Ookubo, H. Yokoyama, H. Kato, T. Araki, Gender differences on MPTP (1-methyl-4-phenyl-1,2,3,6-tetrahydropyridine) neurotoxicity in C57BL/6 mice, Molecular and Cellular Endocrinology 311 (2009) 62–68.
[24] N.N. Rommelse, B. Franke, H.M. Geurts, C.A. Hartman, J.K. Buitelaar, Shared heritability of attention-deficit/hyperactivity disorder and autism spectrum disorder, European Child and Adolescent Psychiatry 19 (2010) 281–295.
[25] S.M. Sato, K.M. Schulz, C.L. Sisk, R.I. Wood, Adolescents and androgens, receptors and rewards, Hormones and Behavior 53 (2008) 647–658.
[26] M.M. Seno, P. Hu, F.G. Gwadry, D. Pinto, C.R. Marshall, G. Casallo, S.W. Scherer, Gene and miRNA expression profiles in autism spectrum disorders, Brain Research 1380 (2011) 85–97.
[27] S. Ueno, Genetic polymorphisms of serotonin and dopamine transporters in mental disorders, Journal of Medical Investigation 50 (2003) 25–31.
[28] S. Ueno, M. Nakamura, M. Mikami, K. Kondoh, H. Ishiguro, T. Arinami, T. Komiyama, H. Mitsushio, A. Sano, H. Tanabe, Identification of a novel polymorphism of the human dopamine transporter (*DAT1*) gene and the significant association with alcoholism, Molecular Psychiatry 4 (1999) 552–557.
[29] D.J. Vandenbergh, A.M. Persico, A.L. Hawkins, C.A. Griffin, X. Li, E.W. Jabs, G.R. Uhl, Human dopamine transporter gene (*DAT1*) maps to chromosome 5p15.3 and displays a VNTR, Genomics 14 (1992) 1104–1106.
[30] D.J. Vandenbergh, M.D. Thompson, E.H. Cook, E. Bendahhou, T. Nguyen, M.D. Krasowski, D. Zarrabian, D. Comings, E.M. Sellers, R.F. Tyndale, S.R. George, B.F. O'Dowd, G.R. Uhl, Human dopamine transporter gene: coding region conservation among normal, Tourette's disorder, alcohol dependence and attention-deficit hyperactivity disorder populations, Molecular Psychiatry 5 (2000) 283–292.
[31] S.H. VanNess, M.J. Owens, C.D. Kilts, The variable number of tandem repeats element in DATI regulates in vitro dopamine transporter density, BMC Genetics 6 (2005).
[32] M.A. Villaronga, D.N. Lavery, C.L. Bevan, S. Llanos, B. Belandia, HEY1 Leu94Met gene polymorphism dramatically modifies its biological functions, Oncogene 29 (2010) 411–420.
[33] M. Waza, H. Adachi, M. Katsuno, M. Minamiyama, C. Sang, F. Tanaka, A. Inukai, M. Doyu, G. Sobue, 17-AAG, an Hsp90 inhibitor, ameliorates polyglutamine-mediated motor neuron degeneration, Nature Medicine 11 (2005) 1088–1095.

Journal of the Neurological Sciences 318 (2012) 100–105

Contents lists available at SciVerse ScienceDirect

Journal of the Neurological Sciences

journal homepage: www.elsevier.com/locate/jns

Heterozygous UDP-GlcNAc 2-epimerase and *N*-acetylmannosamine kinase domain mutations in the *GNE* gene result in a less severe GNE myopathy phenotype compared to homozygous *N*-acetylmannosamine kinase domain mutations

Madoka Mori-Yoshimura [a,*], Kazunari Monma [b], Naoki Suzuki [c], Masashi Aoki [c], Toshihide Kumamoto [d], Keiko Tanaka [e], Hiroyuki Tomimitsu [f], Satoshi Nakano [g], Masahiro Sonoo [h], Jun Shimizu [i], Kazuma Sugie [j], Harumasa Nakamura [a,k], Yasushi Oya [a], Yukiko K. Hayashi [b], May Christine V. Malicdan [b], Satoru Noguchi [b], Miho Murata [a], Ichizo Nishino [b]

[a] *Department of Neurology, National Center Hospital, National Center of Neurology and Psychiatry, 4-1-1 Ogawahigashi, Kodaira, Tokyo 187-8551, Japan*
[b] *Department of Neuromuscular Research, National Institute of Neuroscience, National Center of Neurology and Psychiatry, 4-1-1 Ogawahigashi, Kodaira, Tokyo 187-8502, Japan*
[c] *Department of Neurology, Tohoku University School of Medicine, 1-1 Seiryo, Aoba-ku, Sendai 980-8574, Japan*
[d] *Department of Internal Medicine 3, Faculty of Medicine, Oita University, 1-1 Idaigaoka, Hasama, Yufu-shi, Oita 879-5593, Japan*
[e] *Department of Neurology, Kanazawa Medical University, 1-1 Daigaku, Uchinadamachi, Kahoku-gun, Ishikawa, 920-0214, Japan*
[f] *Department of Neurology and Neurological Science, Graduate School, Tokyo Medical and Dental University, Yushima 1-5-45, Bunkyo-ku, Tokyo 113-8519, Japan*
[g] *Department of Neurology, Osaka City General Hospital, 2-13-22, Miyakojimahonndoori, Miyakojima-ku, Osaka534-0021, Japan*
[h] *Department of Neurology, Teikyo University School of Medicine, Kaga 2-11-1, Itabashi-ku, Tokyo 173-8605, Japan*
[i] *Department of Neurology, Division of Neuroscience, Graduate School of Medicine, University of Tokyo, 7-3-1 Hongo, Bunkyo-ku, Tokyo 113-8655, Japan*
[j] *Department of Neurology, Nara Medical University School of Medicine, 840 Shijo, Kashihara, Nara 634-8521, Japan*
[k] *Clinical Trial Division, Division of Clinical Research, National Center Hospital of Neurology and Psychiatry, 4-1-1 Ogawahigashi, Kodaira, Tokyo 187-8551, Japan*

ARTICLE INFO

Article history:
Received 10 January 2012
Received in revised form 20 March 2012
Accepted 21 March 2012
Available online 14 April 2012

Keywords:
GNE myopathy
Distal myopathy with rimmed vacuoles
Hereditary inclusion body myopathy
Glucosamine (UDP-N-acetyl)-2-epimerase/*N*-acetylmannosamine kinase
(UDP-N-acetyl)-2-epimerase domain
N-acetylmannosamine kinase domain
Questionnaire
Natural history

ABSTRACT

Background: Glucosamine (UDP-N-acetyl)-2-epimerase/*N*-acetylmannosamine kinase (GNE) myopathy, also called distal myopathy with rimmed vacuoles (DMRV) or hereditary inclusion body myopathy (HIBM), is a rare, progressive autosomal recessive disorder caused by mutations in the *GNE* gene. Here, we examined the relationship between genotype and clinical phenotype in participants with GNE myopathy.
Methods: Participants with GNE myopathy were asked to complete a questionnaire regarding medical history and current symptoms.
Results: A total of 71 participants with genetically confirmed GNE myopathy (27 males and 44 females; mean age, 43.1 ± 13.0 (mean ± SD) years) completed the questionnaire. Initial symptoms (*e.g.*, foot drop and lower limb weakness) appeared at a mean age of 24.8 ± 8.3 years. Among the 71 participants, 11 (15.5%) had the ability to walk, with a median time to loss of ambulation of 17.0 ± 2.1 years after disease onset. Participants with a homozygous mutation (p.V572L) in the *N*-acetylmannosamine kinase domain (KD/KD participants) had an earlier disease onset compared to compound heterozygous participants with mutations in the uridine diphosphate-N-acetylglucosamine (UDP-GlcNAc) 2-epimerase and *N*-acetylmannosamine kinase domains (ED/KD participants; 26.3 ± 7.3 vs. 21.2 ± 11.1 years, respectively). KD/KD participants were more frequently non-ambulatory compared to ED/KD participants at the time of survey (80% vs. 50%). Data were verified using medical records available from 17 outpatient participants.
Conclusions: Homozygous KD/KD participants exhibited a more severe phenotype compared to heterozygous ED/KD participants.

1. Introduction

Glucosamine (UDP-N-acetyl)-2-epimerase/*N*-acetylmannosamine kinase (GNE) myopathy, also known as distal myopathy with rimmed vacuoles (DMRV), Nonaka myopathy (MIM: 605820) or hereditary inclusion body myopathy (HIBM; MIM: 600737), is an early adult-onset, progressive myopathy that affects the tibialis anterior muscle, but spares quadriceps femoris muscles [1,2]. The disease is caused by a mutation in the *GNE* gene, which encodes a bifunctional enzyme [uridine diphosphate-*N*-acetylglucosamine (UDP-GlcNAc) 2-epimerase (GNE) and *N*-acetylmannosamine kinase (MNK)] known to catalyze two rate-limiting reactions involved in cytosolic sialic acid synthesis [3–7]. Mutations in the *GNE* gene result in decreased enzymatic activity *in vitro* by 30–90% [7–10]. Therefore, hyposialylation is thought to

* Corresponding author. Tel.: +81 42 341 2711; fax: +81 42 346 1852.
E-mail address: yoshimur@ncnp.go.jp (M. Mori-Yoshimura).

0022-510X/$ – see front matter © 2012 Elsevier B.V. All rights reserved.
doi:10.1016/j.jns.2012.03.016

contribute to the pathogenesis of GNE myopathy. This is supported by the myopathic phenotype associated with a mouse model expressing the human D176V mutant GNE protein (GNE−/−hGNED176V-Tg) [11]. Muscle atrophy and weakness are prevented by oral treatment with sialic acid metabolites in this mouse model [12].

A phase I clinical trial using oral sialic acid therapy has recently been performed in Japan for the treatment of GNE myopathy (ClinicalTrials.gov; NCT01236898). A similar phase I study is currently underway in the United States (ClinicalTrials.gov; NCT01359319). Natural history and genotype–phenotype correlations need to be established for a successful phase II clinical trial for the treatment of GNE myopathy. However, only a small number of studies have been conducted that review the natural course of this disease. In addition, the presence of genotype–phenotype correlations is controversial in GNE myopathy, with most reports denying significant correlations [7]. In fact, substantial heterogeneity is observed among participants who have the same mutations. For example, few subjects with p.D176V and p.M712T mutations exhibited a normal or very mild phenotype, with disease onset after the age of 60 [3,13]. Furthermore, only a limited number of studies that analyze compound heterozygous patients are available. Nonetheless, such studies report a variable degree of severity [14–17].

To clarify the potential relationship between genotype and clinical phenotype (*i.e.*, age at onset, disease course, and current symptoms) of GNE myopathy, we performed a questionnaire-based survey of participants with confirmed GNE myopathy.

2. Participants and methods

2.1. Study population

We obtained approval for this study from the Medical Ethics Committee of the National Center of Neurology and Psychiatry (NCNP). Seventy-eight participants with known GNE myopathy were seen at 8 hospitals specializing in muscle disorders in Japan and 83 participants (not all genetically diagnosed) from the Participants Association for Distal Myopathies (PADM) were recruited. Participants provided written informed consent prior to completing the questionnaire.

A total of 75 participants completed and returned the questionnaire. Of the 75 participants analyzed, 4 were found to have only one heterozygous mutation. Because single heterozygous mutations have not been confirmed to cause GNE myopathy, these 4 participants were excluded from this study.

2.2. Study design

The present study is a retrospective and cross-sectional analysis, which includes 71 participants with genetically confirmed GNE myopathy. Clinical information was collected from participants using a questionnaire and genetic information was acquired from available medical records.

2.3. Questionnaire

Participants completed a self-reporting questionnaire regarding 1) developmental and past symptoms, 2) past and present ambulatory status, and 3) information about diagnosis and medical services (Supplementary material, original version in Japanese).

To determine developmental history, we collected the following information: 1) trouble before and/or during delivery, 2) body weight and height at birth, 3) age at first gait, 4) exercise performance during nursery, kindergarten, or school, and 5) age at onset and signs of first symptoms. Participants were also asked about the onset of 1) gait disturbance, 2) walking with assistance (*i.e.*, cane and/or orthotics and/or handrails), 3) wheelchair use, 4) loss of ambulation, and 5) current gait performance. With regard to medical history, participants were asked about 1) age at the time of first hospital visit, 2) whether or not they had symptoms at the time of visit, 3) age at the time of final diagnosis, 4) how many hospitals/clinics were visited before final diagnosis, and 5) whether a biopsy was performed.

2.4. Medical record examination

To verify the accuracy of the information provided by each participant, available medical records from 17 participants (23.9%) seen at outpatient clinics at NCNP were examined (9 males and 8 females).

2.5. Data handling and analysis

All variables were summarized using descriptive statistics, which included mean, standard deviation (SD), median, range, frequency, and percentage. Each variable was compared against age, sex, genotype, and domain mutation (*i.e.*, within the UDP-GlcNAc 2-epimerase domain: ED or *N*-acetylmannosamine kinase domain: KD). Student's *t* test was used to compare the means for each participant group (ED/ED, ED/KD and KD/KD participants). Data from the two participant groups were calculated using chi-square contingency table analysis. The time from disease onset to walking with assistance, time from disease onset to wheelchair use, and time from disease onset to loss of ambulation were evaluated using the Kaplan–Meier method with log-rank analysis. Questionnaire reliability was tested using intraclass correlation coefficients (ICCs), and two-sided 95% confidence intervals (CIs) were calculated using a one-way random effects analysis of variance model for inter-rater reliability. All analyses were performed using SPSS for Macintosh (version 18, SPSS Inc., Chicago, IL).

3. Results

3.1. General characteristics

A total of 71 Japanese individuals (27 males and 44 females) participated in the study. The mean age at data collection was 43.1 ± 10.7 years. None of the participants showed developmental abnormalities during infancy or early childhood.

3.2. GNE mutations

Forty-one percent of study participants (n = 29/71) had homozygous mutations, while 59% (n = 42/71) had compound heterozygous mutations (Table 1). Among homozygous participants, 86.2% (n = 25/29) harbored the p.V572L mutation, while the remaining participants had other mutations. No homozygous participants for the p.D176V mutation were identified. Among compound heterozygous participants, 28.5% (n = 12/42) had p.D176V/p.V572L mutations, while the remaining participants had other mutations. With respect to allelic frequency, 50.0% (71/142) were p.V572L, 20.4% (29/142) p.D176V, 3.5% (5/142) p.C13S, 2.8% (4/142) p.M712T, and 2.1% (3/142) p.A630T. All other mutations accounted for 2%. A total of 18.3% (n = 13/71) of participants were homozygous with a mutation in the GNE domain (ED/ED), 39.4% (n = 28/71) of participants were compound heterozygous with a mutation in the GNE domain and one in the MNK domain (ED/KD), and 42.3% (n = 30/71) of participants had a mutation in the MNK domain in both alleles (KD/KD).

3.3. Past and present symptoms

Mean participant age at symptom onset was 25.2 ± 9.2 years (range, 12–58 years; median, 24.5 years). There was no significant difference between males and females for current age, age at disease

Table 1
Genotypes of the GNE myopathy patient population.

		Questionnaire	Outpatients
ED/ED	Total	13	4
	Homozygote	1	0
	p.C13S homozygote	1	
	Compound heterozygote	12	4
	p.C13S/p.M29T	1	1
	p.C13S/p.A631	1	1
	p.D176V/p.F233S	1	1
	p.D176V/p.R306Q	2	
	p.R129Q/p.D176V	1	
	p.R129Q/p.R277C	1	
	p.D27L/p.D176V	1	1
	p.B89S/p.D176V	1	
	p.D176V/p.R246W	1	
	p.D176V/p.R321C	1	
	p.D176V/p.V331A	1	
ED/KD	Total	28	8
	Compound heterozygote	28	8
	p.D176V/p.V572L	12	3
	p.C13S/p.V572L	1	1
	p.D176V/p.I472T	1	1
	p.D176V/p.L603F	1	1
	p.R177C/p.V572L	1	1
	383insT/p.V572L	1	1
	p.D176V/p.G708S	2	
	p.D187G/p.V572L	2	
	p.R8X/p.V572L	1	
	p.D176V/p.G568S	1	
	p.D176V/p.H626R	1	
	p.D176V/p.A630T	1	
	p.I276T/p.V572L	1	
	p.G295D/p.A631V	1	
	p.A600E/p.D176V	1	
KD/KD	Total	30	5
	Homozygote	28	5
	p.V572L homozygote	25	4
	p.M712T homozygote	2	
	p.A630T homozygote	1	
	Compound heterozygote	2	0
	p.V572L/p.R420X	1	1
	1756Gdel (stop)/p.V572L	1	

onset, age at walking with assistance, age at wheelchair use, and current ambulatory status. Initial symptoms included gait disturbance (66.2%, n = 47/71), other lower limb symptoms (26.8%, n = 19/71), easily fatigued (23.9%, n = 17/71), and weakness of hands and fingers (8.5%, n = 6/71). In addition, 21.1% (n = 15/71) had onset of symptoms before the age of 20. When specifically asked, 47.8% (n = 34/71) described themselves as slow runners during childhood, and 42.5% reported having had difficulty with physical exercise during school years.

3.4. Diagnosis

Mean participant age at diagnosis was 33.9 ± 12.6 years (median, 29.5 years; range 17 to 67 years). Mean participant age at first physician visit was 29.6 ± 10.4 years (median, 27 years; range, 12–62 years), and mean time between first visit and diagnosis was 4.4 ± 8.3 years.

3.5. Walking with assistance and wheelchair use

At the time of the survey, 52.0% (n = 37/71) were ambulant (41.3 ± 12.8 years); however, only 15.5% (n = 11/71, 40.0 ± 13.6 years) could walk without assistance, with the remaining 35.2% requiring assistance (n = 25/71, 41.8 ± 12.7 years). Only 7.0% of these participants (n = 5/71) could walk up stairs, while 49.3% (n = 35/71) were non-ambulant. Wheelchairs were used by 63.6% (23.9% partially bound and 43.7% totally bound) and an electric wheelchair was used by 41.9% (n = 31/71). Mean participant age of wheelchair users was 34.9 ± 11.7 years (range, 18–70 years). Wheelchairs were not used by 32.4% (n = 26/71) of participants. Current age of wheelchair-free participants was 39.4 ± 12.3 years (range, 21–61 years; median, 34 years) and that of wheelchair-bound participants was 42.8 ± 12.6 years (range, 21–71; median, 42 years).

Kaplan–Meier analysis revealed a median proportional age at walking with assistance of 30.0 ± 1.4 years. Median proportional age of wheelchair users was 36.0 ± 2.7 years, and that for loss of ambulation was 45.0 ± 4.2 years. The time from disease onset to walking with assistance was 7.0 ± 0.4 years, time from disease onset to wheelchair use was 11.5 ± 1.2 years, and time from disease onset to loss of ambulation was 17.0 ± 2.1 years.

3.6. Correlation between disease genotype and phenotype

To determine if a correlation between genotype and phenotype existed, we compared domain mutations (ED/KD, or both) available from medical reports to questionnaire answers (Table 2). Participants with KD/KD mutations (both homozygous and heterozygous) were younger and more severely affected compared to participants with ED/KD or ED/ED mutations. No significant difference in current age or age at disease onset between ED/ED and ED/KD participants was identified. Kaplan–Meier analyses revealed that the proportional time from disease onset to wheelchair use and from disease onset to loss of ambulation was significantly shorter in KD/KD compared to ED/KD participants. ED/ED participants exhibited a shorter time of disease onset to wheelchair use compared to ED/KD participants (Table 3, Fig. 1).

3.7. Comparison between p.V572L homozygous and p.D176V/p.V572L compound heterozygous participants

To compare clinical features in patients with the same mutations, we specifically analyzed data from those with p.V572L (n = 25/71, 35.2%) and p.D176V/p.V572L (n = 12/71, 16.9%) mutations, as these two were the most frequent mutations in our study population (Table 2). Age at disease onset of homozygous participants (p.V572L) was 21.3 ± 5.7 years (range, 12–32 years) and time from disease onset to wheelchair use was 11.3 ± 5.4 years (range, 3–21 years). Only 16.0% (n = 4/25) of these homozygous participants reported that they were not currently using a wheelchair. In contrast, the mean age at disease onset of heterozygous participants (p.D176V/p.V572L) was 35.5 ± 14.1 years (range, 13.5–57 years) and time from disease onset to wheelchair use was 17.9 ± 7.0 years (range, 11–28 years). A total of 66.7% of these compound heterozygous participants (n = 8/12) reported that they were not using a wheelchair.

3.8. Questionnaire response compared to medical records

Questionnaires from 17 participants (NCNP outpatient participants) were compared to available medical records (Table 2). Age at disease onset, age at onset of gait disturbance, age at walking with assistance, and age at loss of ambulation were assessed for inter-rater reliability. Age at disease onset, age at onset of gait disturbance, age at walking with assistance, and age at loss of ambulation were assessed for inter-rater reliability. ICC values were 0.979 (95% CI 0.941–0.992) for age at disease onset, 0.917 (95% CI 0.752–0.972) for age at onset of gait disturbances, 0.985 (95% CI 0.949–0.995) for age at walking with assistance, and 0.967 (95% CI 0.855–0.993) for age at loss of ambulation.

4. Discussion

The present study provides a detailed overview of disease severity and progression in 71 Japanese participants with genetically confirmed GNE myopathy. Questionnaire-based surveys have been used to study

Table 2
Comparison of disease course among genotypes.

		Total	ED/ED	ED/LD	KD/KD
Questionnaire	*n*	71	13	28	30
	Age (years old)	43.1 ± 10.7	44.2 ± 11.2	45.3 ± 13.4	40.6 ± 13.0
	Age at onset (years old)	25.5 ± 9.2	26.3 ± 7.3^{+}	29.8 ± 11.0*	21.2 ± 5.5$^{*,+}$
	Age at walking with assistance	31.8 ± 10.0	34.0 ± 11.1	35.6 ± 10.9*	27.8 ± 6.8*
	Duration from onset to walking with assistance	8.4 ± 6.5	7.5 ± 7.3	9.2 ± 6.5	8.0 ± 6.6
	Wheelchair user (%)	48 (67.8)	10(76.9)	14 (50.0)*	24 (80.0)*
	Wheelchair use since (age)	37.6 ± 8.6	36.4 ± 12.0	43.0 ± 8.7*	31.2 ± 9.3*
	Number of patients with lost ambulation	35 (49.8)	6(46.2)	8 (28.6)*	21 (70.0)*
	Age at lost ambulation	33.6 ± 9.2	31.2 ± 6.0	39.7 ± 9.5	32.1 ± 9.3
	Duration from onset to loss of ambulation	12.2 ± 5.2	9.8 ± 3.5	13.8 ± 6.4	12.4 ± 5.1
NCNP outpatients	*n*	17	4	8	5
	Age (years old)	43.9 ± 14.1	53.5 ± 8.9^{+}	44.3 ± 16.3	35.6 ± 9.2^{+}
	Age at onset (years old)	25.8 ± 9.2	33.4 ± 9.2^{+}	29.6 ± 13.5	19.6 ± 4.2^{+}
	Duration from onset to walking with assistance	7.5 ± 4.2	8.9 ± 5.1	8.1 ± 4.7	5.2 ± 1.5
	Wheelchair user (%)	12 (70.6)	3 (75.0)	4 (50.0)	4 (100)
	Wheelchair use since (age)	33.3 ± 12.6	47.5 ± 17.7	35.2 ± 12.4	25.8 ± 6.3
	Number of patients with lost ambulation	9 (52.9)	3 (75.0)	3 (28.6)*	5 (100)*
	Age at lost ambulation	33.8 ± 9.3	40.0 ± 0.0	39.0 ± 16.5	31.0 ± 8.2
	Duration from onset to loss of ambulation	10.7 ± 4.2	11.2 ± 5.6	11.1 ± 7.8	6.2 ± 2.6

In the questionnaire group, age at onset and age at walking with assistance were significantly younger in KD/KD patients than in ED/KD patients. The number of wheelchair users and patients with loss of ambulation was significantly higher in the KD/KD group than in the ED/KD group. In contrast, with the exception of age at onset, there were no significant differences between ED/ED and ED/KD or KD/KD patients in these clinical parameters. The ED/ED patients were older than the others, and KD/KD patients tended to show the fastest progression.

* $p<0.05$ between ED/KD and KD/KD.

$^{+}$ $p<0.05$ between ED/ED and KD/KD.

the natural disease course of other rare neuromuscular disorders, such as Pompe disease [18] and spinal muscular atrophy type-1 [19]. It is difficult to establish the natural history of such rare disorders using medical records only because patients are typically seen in many different hospitals. In the present study, we used a self-reporting questionnaire and support its use for complementing medical records because it provides a more complete disease overview and establishes specific clinical trends or correlations. Indeed, our questionnaire demonstrates excellent inter-rater reliability against medical records and yields several findings regarding differences in disease progression among genetically distinct, GNE myopathy participants.

Only 15.5% of participants could walk and 7.0% could walk up stairs without assistance, which reflects the fact that GNE myopathy patients often require canes and/or leg braces at an early disease stage. This indicates that traditional six-minute walk or four-step walking tests often used to evaluate muscular dystrophies or myopathies can only be applied in a very limited number of cases, such as natural disease course studies or clinical trials. Therefore, alternate evaluation tools are required, which should include functional measurements that can be completed without canes or braces. For example, the Gross Motor Function Measure is a useful tool for evaluating mildly and severely affected patients [20].

The male to female ratio in our study population (27 males and 44 females) was skewed from the expected ratio for autosomal recessive inheritance. However, the male to female ratio of the 17 NCNP outpatient participants was 9:8. One possible explanation for the observed sex ratio in our study population is that female participants tend to be more enthusiastic toward questionnaire-based and/or PADM activities. There was no significant difference in age at survey and age at disease onset between male and female participants. However, in a mouse model of GNE myopathy, weight loss and muscle atrophy were more pronounced and occurred earlier in females compared to males [11].

We showed that KD/KD mutations are associated with a more severe phenotype compared to ED/KD mutations. Indeed, KD/KD participants had an earlier disease onset, a more rapid and progressive disease course, and a shorter time from disease onset to loss of ambulation. This was also observed in the 17 NCNP outpatient participants analyzed in our study. In contrast, ED/ED participants did not show significant differences across disease course parameters analyzed except for an earlier and later age at disease onset compared to ED/KD and KD/KD participants, respectively. Thus, ED/ED participants appear to have a disease severity intermediate between ED/KD and KD/KD participants. One possible explanation is that the major mutation, p.V572L, may be associated with a more severe phenotype. In general, the reasons for this earlier onset and disease progression remain unknown. Jewish GNE myopathy patients with homozygous p.M712T mutations have a milder phenotype compared to Japanese patients, as most of their quadriceps are spared and they usually become wheelchair-bound 15 years or more after disease onset [13,21]. Our study population included two women with homozygous p.M712T mutations: a 38 year-old ambulant and a 35 year-old non-ambulant participant. Although the two participants had a slightly later disease onset (ages 23 and 27 years, respectively) compared to KD/KD participants, the difference was not significant.

An asymptomatic patient with a p.D176V homozygous mutation was previously reported [3]. The study suggested that p.D176V homozygous patients may show a mild or late disease onset phenotype. The results presented here may support this observation as no p.D176V homozygous participants were present in our study

Table 3
Inter-rater reliability of the questionnaire.

	Onset	Age of gait disturbance	Age of gait with help	Age at loss of ambulant
Number of patients	17	17	13	9
ICC (95% CI)	0.979 (0.941–0.992)	0.917 (0.752–0.972)	0.985 (0.949–0.995)	0.967 (0.855–0.993)
p	0.000	0.000	0.000	0.000

Age at onset, age at onset of gait disturbances, age at walking with assistance, and age at loss of ambulation were assessed in a subgroup of 17 outpatients to evaluate the inter-rater reliability of the questionnaire.

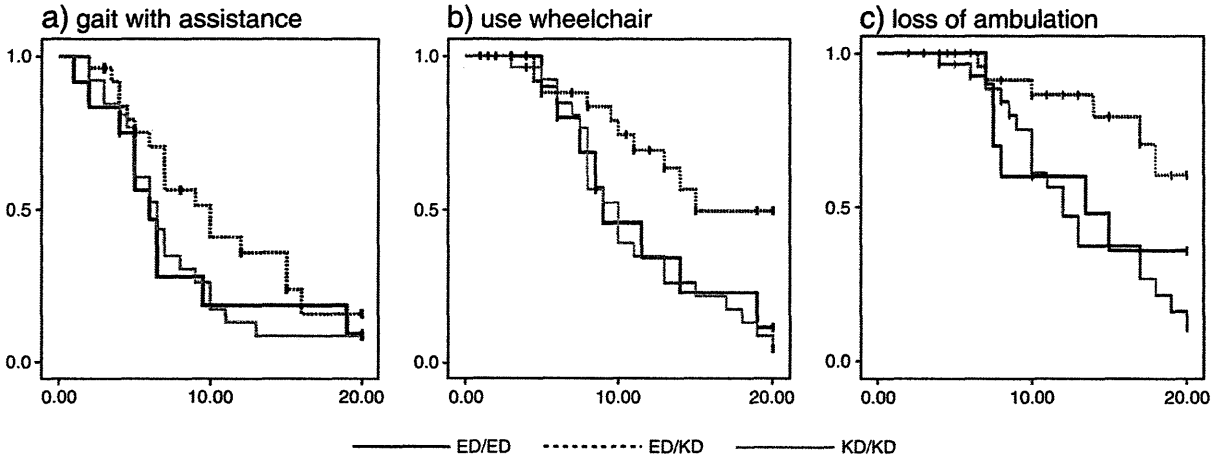

Fig. 1. Kaplan–Meier analysis of time from disease onset to (a) walking with assistance, (b) wheelchair use, and (c) loss of ambulation. Significant differences between ED/KD and KD/KD genotypes were identified. Age at disease onset was significantly different between ED/ED participants and ED/KD and KD/KD participants.

population, although p.D176V was the second most common mutation carried by 29 of our participants. In addition, a high variability was observed regarding age at disease onset and disease progression, underscoring the role of a yet-to-be identified factor(s) in determining disease phenotype.

The recruitment of participants from PADM and highly specialized neurology hospitals is a potential source of selection bias and thus a limitation of this study. These participants are likely to be more motivated because they are more severely affected compared to the general patient population. Furthermore, patients with lower disease severity may not yet be diagnosed with GNE myopathy. Therefore, our study may not accurately reflect the general patient population. Nevertheless, we believe our findings provide important information as our study population covers a broad range in age (22 to 81 years) and symptoms (minimal to wheelchair-bound). Finally, recall bias may also affect results presented in this retrospective study. Therefore, future studies should be performed with an emphasized prospective design.

In conclusion, our study shows that the KD/KD genotype (*i.e.*, p.V572L homozygous mutation) is associated with a more severe phenotype compared to compound heterozygous ED/KD mutations. Because only a small number of participants could walk, future studies should include ambulation-independent motor tests to yield a more comprehensive clinical overview in GNE myopathy patients with different genotypes.

Supplementary data to this article can be found online at doi:10.1016/j.jns.2012.03.016.

Conflict of interest

We certify that there is no conflict of interest with any financial organization regarding the material discussed in the manuscript.

Acknowledgments

We thank members of the Patients Association for Distal Myopathies (PADM) for their help. This work was partly supported by the Research on Intractable Diseases of Health and Labor Sciences Research Grants; Comprehensive Research on Disability Health and Welfare Grants, Health and Labor Science Research Grants; Intramural Research Grant (23-4, 23-5) for Neurological and Psychiatric Disorders of NCNP; and a Young Investigator Fellowship from the Translational Medical Center, NCNP.

References

[1] Nonaka I, Sunohara N, Satoyoshi E, Terasawa K, Yonemoto K. Autosomal recessive distal muscular dystrophy: a comparative study with distal myopathy with rimmed vacuole formation. Ann Neurol 1985;17:51–9.
[2] Argov Z, Yarom R. "Rimmed vacuole myopathy" sparing the quadriceps. A unique disorder in Iranian Jews. J Neurol Sci 1984;64:33–43.
[3] Nishino I, Noguchi S, Murayama K, Driss A, Sugie K, Oya Y, et al. Distal myopathy with rimmed vacuoles is allelic to hereditary inclusion body myopathy. Neurology 2002;59:1689–93.
[4] Eisenberg I, Avidan N, Potikha T, Hochner H, Chen M, Olender T, et al. The UDP-N-acetylglucosamine 2-epimerase/N-acetylmannosamine kinase gene is mutated in recessive hereditary inclusion body myopathy. Nat Genet 2001;29:83–7.
[5] Kayashima T, Matsuo H, Satoh A, Ohta T, Yoshiura K, Matsumoto N, et al. Nonaka myopathy is caused by mutations in the UDP-N-acetylglucosamine-2-epimerase/N-acetylmannosamine kinase gene (GNE). J Hum Genet 2002;47:77–9.
[6] Keppler OT, Hinderlich S, Langner J, Schwartz-Albiez R, Reutter W, Pawlita M. UDP-GlcNAc 2-epimerase: a regulator of cell surface sialylation. Science 1999;284:1372–6.
[7] Malicdan MC, Noguchi S, Nishino I. Recent advances in distal myopathy with rimmed vacuoles (DMRV) or hIBM: treatment perspectives. Curr Opin Neurol 2008;21:596–600.
[8] Noguchi S, Keira Y, Murayama K, Ogawa M, Fujita M, Kawahara G, et al. Reduction of UDP-N-acetylglucosamine 2-epimerase/N-acetylmannosamine kinase activity and sialylation in distal myopathy with rimmed vacuoles. J Biol Chem 2004;279:11402–7.
[9] Broccolini A, Gidaro T, De Cristofaro R, Morosetti R, Gliubizzi C, Ricci E, et al. Hyposialylation of neprilysin possibly affects its expression and enzymatic activity in hereditary inclusion–body myopathy muscle. J Neurochem 2008;105:971–81.
[10] Salama I, Hinderlich S, Shlomai Z, Eisenberg I, Krause S, Yarema K, et al. No overall hyposialylation in hereditary inclusion body myopathy myoblasts carrying the homozygous M712T GNE mutation. Biochem Biophys Res Commun 2005;328:221–6.
[11] Malicdan MC, Noguchi S, Nonaka I, Hayashi YK, Nishino I. A Gne knockout mouse expressing human GNE D176V mutation develops features similar to distal myopathy with rimmed vacuoles or hereditary inclusion body myopathy. Hum Mol Genet 2007;16:2669–82.
[12] Malicdan MC, Noguchi S, Hayashi YK, Nonaka I, Nishino I. Prophylactic treatment with sialic acid metabolites precludes the development of the myopathic phenotype in the GNE myopathy mouse model. Nat Med 2009;15:690–5.
[13] Argov Z, Eisenberg I, Grabov-Nardini G, Sadeh M, Wirguin I, Soffer D, et al. Hereditary inclusion body myopathy: the Middle Eastern genetic cluster. Neurology 2003;60:1519–23.
[14] Tomimitsu H, Shimizu J, Ishikawa K, Ohkoshi N, Kanazawa I, Mizusawa H. Distal myopathy with rimmed vacuoles (DMRV): new GNE mutations and splice variant. Neurology 2004;11:1607–10.
[15] Yabe I, Higashi T, Kikuchi S, Sasaki H, Fukazawa T, Yoshida K, et al. GNE mutations causing distal myopathy with rimmed vacuoles with inflammation. Neurology 2003;12:384–6.
[16] Chu CC, Kuo HC, Yeh TH, Ro LS, Chen SR, Huang CC. Heterozygous mutations affecting the epimerase domain of the GNE gene causing distal myopathy with rimmed vacuoles in a Taiwanese family. Clin Neurol Neurosurg 2007;109:250–6.
[17] Ro LS, Lee-Chen GJ, Wu YR, Lee M, Hsu PY, Chen CM. Phenotypic variability in a Chinese family with rimmed vacuolar distal myopathy. J Neurol Neurosurg Psychiatry 2005;76:752–5.

[18] Hagemans ML, Winkel LP, Van Doorn PA, Loonen MC, Hop WJ, Reuser AJ, et al. Clinical manifestation and natural course of late-onset Pompe's disease in 54 Dutch patients. Brain 2005;128:671–7.
[19] Oskoui M, Levy G, Garland CJ, Gray JM, O'Hagen J, De Vivo DC, et al. The changing natural history of spinal muscular atrophy type 1. Neurology 2007;69: 1931–6.
[20] Sienko Thomas S, Buckon CE, Nicorici A, Bagley A, McDonald CM, Sussman MD. Classification of the gait patterns of boys with Duchenne muscular dystrophy and their relationship to function. J Child Neurol 2010;25:1103–9.
[21] Eisenberg I, Grabov-Nardini G, Hochner H, Korner M, Sadeh M, Bertorini T, et al. Mutations spectrum of GNE in hereditary inclusion body myopathy sparing the quadriceps. Hum Mutat 2003;21:99.

PLOS | CURRENTS MUSCULAR DYSTROPHY

The C2A domain in dysferlin is important for association with MG53 (TRIM72)

November 5, 2012 · Advanced Diagnostics and Biomarkers

Chie Matsuda[1], Katsuya Miyake, Kimihiko Kameyama[2], Etsuko Keduka[3], Hiroshi Takeshima[4], Toru Imamura[5], Nobukazu Araki[6], Ichizo Nishino[7], Yukiko Hayashi[8]

1 Biomedical Research Institute, National Institute of Advanced Industrial Science and Technology; Department of Neuromuscular Research, National Institute of Neuroscience, National Center of Neurology and Psychiatry, **2** Biomedical Research Institute, National Institute of Advanced Industrial Science and Technology, **3** Department of Neuromuscular Research, National Institute of Neuroscience, National Center of Neurology and Psychiatry, **4** Department of Biological Chemistry, Kyoto University Graduate School of Pharmaceutical Science, **5** Biomedical Research Institute, National Institute of Advanced Industrial Science and Technology, **6** Department of Histology and Cell Biology, School of Medicine, Kagawa University, **7** Department of Neuromuscular Research, National Institute of Neuroscience, National Center of Neurology and Psychiatry; Department of Clinical Development, Translational Medical Center, National Center of Neurology and Psychiatry, **8** Department of Neuromuscular Research, National Institute of Neuroscience, National Center of Neurology and Psychiatry; Department of Clinical Development, Translational Medical Center, National Center of Neurology and Psychiatry

Matsuda C, Miyake K, Kameyama K, Keduka E, Takeshima H, Imamura T, Araki N, Nishino I, Hayashi Y. The C2A domain in dysferlin is important for association with MG53 (TRIM72). PLOS Currents Muscular Dystrophy. 2012 Nov 5 [last modified: 2012 Nov 5]. Edition 1. doi: 10.1371/5035add8caff4.

Abstract

In skeletal muscle, Mitsugumin 53 (MG53), also known as muscle-specific tripartite motif 72, reportedly interacts with dysferlin to regulate membrane repair. To better understand the interactions between dysferlin and MG53, we conducted immunoprecipitation (IP) and pull-down assays. Based on IP assays, the C2A domain in dysferlin associated with MG53. MG53 reportedly exists as a monomer, a homodimer, or an oligomer, depending on the redox state. Based on pull-down assays, wild-type dysferlin associated with MG53 dimers in a Ca2+-dependent manner, but MG53 oligomers associated with both wild-type and C2A-mutant dysferlin in a Ca2+-independent manner. In pull-down assays, a pathogenic missense mutation in the C2A domain (W52R-C2A) inhibited the association between dysferlin and MG53 dimers, but another missense mutation (V67D-C2A) altered the calcium sensitivity of the association between the C2A domain and MG53 dimers. In contrast to the multimers, the MG53 monomers did not interact with wild-type or C2A mutant dysferlin in pull-down assays. These results indicated that the C2A domain in dysferlin is important for the Ca2+-dependent association with MG53 dimers and that dysferlin may associate with MG53 dimers in response to the influx of Ca2+ that occurs during membrane injury.

To examine the biological role of the association between dysferlin and MG53, we co-expressed EGFP-dysferlin with RFP-tagged wild-type MG53 or RFP-tagged mutant MG53 (RFP-C242A-MG53) in mouse skeletal muscle, and observed molecular behavior during sarcolemmal repair; it has been reported that the C242A-MG53 mutant forms dimers, but not oligomers. In response to membrane wounding, dysferlin accumulated at the injury site within 1 second; this dysferlin accumulation was followed by the accumulation of wild-type MG53. However, accumulation of RFP-C242A MG53 at the wounded site was impaired relative to that of RFP-wild-type MG53. Co-transfection of RFP-C242A MG53 inhibited the recruitment of dysferlin to the sarcolemmal injury site. We also examined the molecular behavior of GFP-wild-type MG53 during sarcolemmal repair in dysferlin-deficient mice which show progressive muscular dystrophy, and found that GFP-MG53 accumulated at the wound similar to

wild-type mice. Our data indicate that the coordination between dysferlin and MG53 plays an important role in efficient sarcolemmal repair.

Funding Statement

This study was partly supported by intramural Research Grant 23-4 (YKH) and 23-5 (CM, IN) for Neurologicaland Psychiatric Disorders of NCNP; partly by Research on Intractable Diseases, Comprehensive Research on Disability Health and Welfare (YKH, IN), and Applying Health Technology from the Ministry of Health Labour and Welfare (IN); and partly by JSPS KAKENHI Grant Numbers of 18590966 (CM), 24390227 (YKH), and 24659437 (YKH).

Introduction

Dysferlin is a sarcolemmal protein, and dysferlin deficiency causes Miyoshi myopathy (MM) and limb girdle muscular dystrophy type 2B (LGMD2B) [1,2]. Based on the observation that dysferlin accumulates at wound sites in myofibers in a Ca^{2+}-dependent manner, dysferlin is thought to mediate Ca^{2+}-dependent sarcolemmal repair [3].

Mitsugumin 53 (MG53), also known as muscle-specific tripartite motif 72, is a recently identified protein involved in membrane repair in skeletal muscle [4]. Mice lacking MG53 suffer progressive myopathy [4], similar to dysferlin-null mice [3]. MG53 is localized in intracellular vesicles and plasma membranes in skeletal muscle, and it accumulates at injury sites in an oxidation-dependent, but not Ca^{2+}-dependent, manner [4].

MG53 interacts with dysferlin and caveolin-3 to regulate sarcolemmal repair [5]. When expressed in C2C12 myoblasts that lack endogenous MG53, damaged membrane sites cannot be repaired in the presence of GFP-dysferlin, however, co-transfection of MG53 and GFP-dysferlin in these myoblasts results in GFP-dysferlin accumulation at injury sites [5]. These findings indicated that recruitment of dysferlin to the injury site of the membrane depends on MG53. However, it remains unclear whether the absence of dysferlin perturbs recruitment of MG53 to the injury site for membrane repair. A previous report has demonstrated the association of dysferlin with MG53 with co-immunoprecipitation (IP) assays using mouse skeletal muscle and C2C12 myoblasts transfected with dysferlin and MG53 [5]. However, which protein domains participate in this interaction between dysferlin and MG53 and whether this interaction is dependent on Ca^{2+} remain unclear. MG53 oligomerizes via disulfide bonds [4] and forms homodimers via a leucine-zipper motif in the coiled-coil domain [6]. The interaction between dysferlin proteins and MG53 monomers or oligomers has not been characterized in detail. To understand the precise role of dysferlin and MG53 in sarcolemmal repair, it would be helpful to determine whether dysferlin associates with MG53 monomers, oligomers, or both in a Ca^{2+}-dependent manner.

Thus, to examine the biological role of the association between dysferlin and MG53, we used the following strategy to examine the effect of the absence of MG53 oligomers on dysferlin. We co-transfected mouse skeletal muscle with wild-type dysferlin-EGFP and RFP-tagged wild-type MG53 or a RFP-tagged MG53 mutant (RFP-C242A -MG53), and conducted a membrane-repair assay using a two-photon laser microscope. The C242A-MG53 mutant has been reported to form dimers, but not oligomers [6]. There is no report of simultaneous observation of dysferlin and MG53 during sarcolemmal repair; however, we have successfully performed real-time imaging of dysferlin-GFP and MG53-RFP after membrane injury in mouse skeletal muscle.

Dysferlin protein is absent or severely reduced in the skeletal muscle of patients with dysferlinopathy [7] and of SJL and A/J mice with mutations in the dysferlin genes [8]. To examine whether the absence of dysferlin affects the recruitment of MG53 to injury sites, we transfected skeletal muscle from dysferlin-deficient SJL and A/J mice with EGFP-MG53 and conducted membrane repair assays. These experiments are helpful in elucidating the

molecular pathology of dysferlinopathy and revealed that MG53 accumulated in the skeletal muscles of dysferlin-deficient mice, which develop progressive muscular dystrophy.

We present evidence indicating that efficient sarcolemmal repair requires both dysferlin and MG53.

Methods

Immunoprecipitation. To examine the interaction between MG53 and dysferlin, mouse gastrocnemius muscles were lysed in lysis buffer containing 20 mM Tris-HCl (pH 7.5), 150 mM NaCl, 1% NP-40, and Complete mini EDTA-free protease inhibitor cocktail (Roche) [9] supplemented with 1 mM $CaCl_2$ or 2 mM EGTA. Lysates pre-cleared with Protein A/G agarose (Pierce) were incubated with polyclonal antibodies against mouse MG53 [4] or mouse dysferlin; the anti-dysferlin antibody was made in rabbit by injecting bacterial recombinant protein containing residues 1669 to 1790. The immunoprecipitated proteins were separated by SDS-PAGE and detected on immunoblots using the same antibodies used for IP or the anti-human dysferlin monoclonal antibody, NCL-Hamlet (Novocastra Laboratories).

A human MG53 cDNA was amplified by PCR and subcloned into pFLAG-CMV-4 (Sigma). Wild-type and truncated human dysferlin that were each tagged with c-myc were generated previously [10]. We also created five truncated human dysferlin constructs with the C2A domain (aa 1-149, 1-349, and 1-1080) and without the C2A domain (aa 130-2080 and 1081-2080). The sequence of each construct was verified by DNA sequencing. FuGENE 6 or E-xtremeGENE 9 (Roche) was used to transiently transfect COS-7 cells with MG53 and wild-type or mutant dysferlin constructs. Transfectants were cultured for 48 h and subsequently lysed in the same lysis buffer used to lyse mouse muscle, except that this buffer lacked $CaCl_2$ and EGTA. Lysates pre-cleared with Protein G-Sepharose (GE Healthcare) were incubated with anti-FLAG (M2, Sigma) or anti-c-myc (9E10, Santa Cruz Biotechnology) monoclonal antibodies; Protein G-Sepharose was then added. Immunoprecipitated proteins were analyzed by immunoblotting using M2 and anti-c-myc polyclonal (A14, Santa Cruz Biotechnology) antibodies.

Pull-down assay. Fragments of the dysferlin C2A domain (corresponding to aa 1-129 of human dysferlin) were amplified as cDNA by PCR and subcloned into pGEX-5X-3 (GE Healthcare). Dysferlin p.W52R (TGG to CGG at c.527-529) and p.V67D (GTG to GAT at c.572-574) mutations were introduced by PCR using appropriate primers. GST fusion proteins expressed in BL21 *E. coli* were purified using sarkosyl [11] and bound to glutathione Sepharose 4B (GE Healthcare). COS-7 cells overexpressing FLAG-tagged human MG53 were lysed in lysis buffer containing 10 mM Na_2HPO_4, 1.8 mM KH_2HPO_4, 1% NP-40 (pH 7.4), 2 mM EGTA, various concentration of $CaCl_2$, and Complete mini EDTA-free protease inhibitor cocktail. EGTA was used to chelate the free Ca^{2+} in solution and $CaCl_2$ at various concentrations. The free calcium concentration was calculated using the free software CALCON3.6. Lysates were centrifuged to remove cellular debris, supplemented with 5 mM N-methylmaleimide (NEM) or 5 mM dithiothreitol (DTT), and finally subjected to protein cross-linking by treating with 2 mM glutaraldehyde (GA) for 5 min at room temperature, which was quenched with 100 mM Tris-HCl (pH 7.5) [6]. The cross-linked lysates were diluted with 75 mM Tris-HCl (pH 7.5), 150 mM NaCl, 1% NP-40, 2 mM EGTA, various concentrations of $CaCl_2$, and Complete mini EDTA-free protease inhibitor cocktail. Lysates pre-cleared with GST bound to glutathione Sepharose 4B were divided into aliquots and incubated with wild-type, p.W52R, and p.V67D dysferlin C2A-GST fusion protein bound to beads for 2 hr at 4°C. After three washes in lysis buffer containing 75 mM Tris-HCl (pH 7.5), 2× sample buffer (125 mM Tris-HCl (pH 6.8), 4% SDS, 20% (v/v) glycerol, and 0.004% bromophenol blue) was added to the beads, and the mixtures were incubated for 10 min at 85°C. Bound proteins were separated by SDS-PAGE and subjected to immunoblotting with the anti-FLAG antibody M2.

In vivo transfection and membrane repair assay. Twenty micrograms of N-terminal RFP-tagged human MG53 cDNA/pcDNA3.1 and/or C-terminal GFP-tagged human dysferlin cDNA/pcDNA3.1 plasmid DNA were injected into

the flexor digitorum brevis of anesthetized, 4-week-old male C57BL6J and dysferlin-deficient SJL and A/J mice. Electroporation of plasmid DNA was performed using an electric pulse generator (CUY21SC, NEPAGENE) as described previously [12]. Seven days after electroporation, skeletal muscle myocytes (for whole-mount viewing) or individual myofibers were isolated and subjected to plasma membrane injury created by a two-photon laser microscope, LSM 710NLO with GaAsp Detectors (Zeiss) and Chameleon Vision II System (Coherent)[3]. Myofiber wounding using the 820-nm infrared laser and resealing analysis based on the kinetics and extent of FM1-43 or 4-46 dye (Molecular Probes) entry through open disruptions was carried out as previously described [3,13,14].

Ethics Statement. All experiments involving animals were performed according to the Procedure for Handling Experiments involving Animals of AIST (National Institute of Advanced Industrial Science and Technology) and approved by the Institutional Animal Care and Use Committee of AIST.

Results

Association of MG53 and dysferlin in mouse skeletal muscle

We used an IP assay with protein from mouse muscle to confirm that endogenous MG53 associates with dysferlin *in vivo*. MG53 and dysferlin associated only in the absence of EGTA and $CaCl_2$ (Fig. 1). The same result was obtained using C2C12 myotubes (data not shown). MG53 was specifically co-immunoprecipitated by the anti-dysferlin antibody, and conversely dysferlin was specifically co-immunoprecipitated by the anti-MG53 antibody. Thus, we confirmed that endogenous MG53 and endogenous dysferlin form a protein complex in mouse skeletal muscle without EGTA or $CaCl_2$ supplementation.

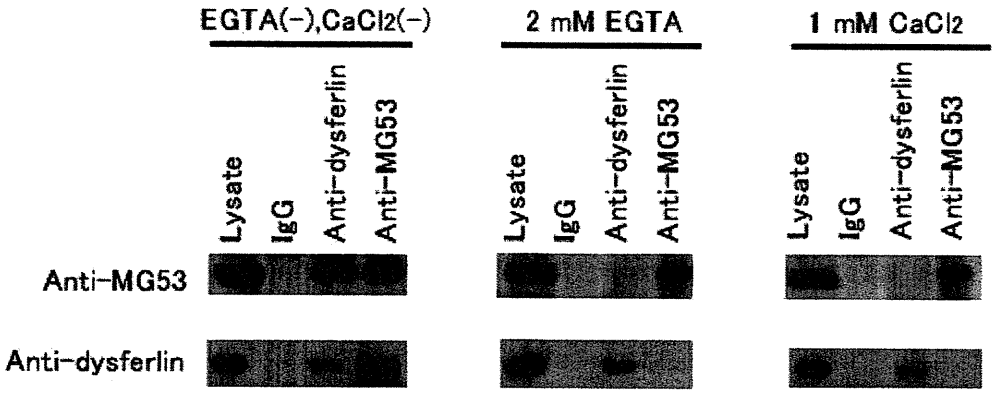

Fig. 1: IP assay of dysferlin and MG53.

MG53interacts with dysferlin in mouse skeletal muscle. Extracts from wild-type mouse skeletal muscle were subjected to IP with polyclonal anti-MG53 antibodies or polyclonal anti-dysferlin antibodies. Immunoprecipitated proteins were subjected to SDS-PAGE and visualized on immunoblots treated with the same antibodies that were used for IP.

Identification of the MG53-associating domain of dysferlin

Next, we used IP to define the region of dysferlin that associates with MG53. Specifically, we used transient co-transfection to introduce a construct encoding full-length human MG53 tagged with FLAG and a construct encoding human dysferlin tagged with c-myc into COS-7 cells; for each co-transfection, full-length dysferlin or one of five deletion mutant forms of tagged dysferlin was used (Fig. 2). For deletion mutants that lacked the C-terminal domain of dysferlin, the transmembrane domain of dysferlin was retained to increase protein stability [10]. Transfectants were lysed in the same buffer that was used for IP assays of mouse skeletal muscle extract, except that this buffer lacked EGTA and $CaCl_2$. Full-length dysferlin and deletion mutants that retained the N-terminal C2 (C2A) domain of dysferlin were co-immunoprecipitated by anti-MG53 antibody. In contrast, dysferlin mutants that lacked this N-terminal domain, Δ2-1080 and Δ2-129, failed to interact with MG53. These results indicated that the C2A domain of dysferlin was necessary for association with MG53.